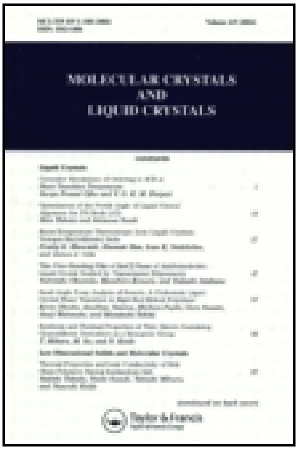

Molecular Crystals and Liquid Crystals
Publication details, including instructions for authors and subscription information:
http://www.tandfonline.com/loi/gmcl16

The Influence of Material and Device Parameters on the Optical Characteristics of Liquid Crystal Displays

G. Baur [a]
[a] Fraunhofer-Institut für Angewandte Festkörperphysik (IAF), Freiburg, D-7800, W. Germany

Version of record first published: 14 Oct 2011.

Mol. Cryst. Liq. Cryst., 1981, Vol. 63, pp. 45–58
0026-8941/81/6304–0045 $06.50/0

The Influence of Material and Device Parameters on the Optical Characteristics of Liquid Crystal Displays†

G. BAUR

Fraunhofer-Institut für Angewandte Festkörperphysik (IAF) D-7800 Freiburg, W. Germany.

(*Received November 3, 1980*)

A review of the influence of material and cell parameters on the optical characteristics of TN-displays is given. The optical response is dependent on the elastic constants, the dielectric constants, the viscosities, and the combination of cell thickness and refractive index anisotropy. Model calculations of the optical characteristics of TN-cells for different combinations of material and cell parameters are presented.

INTRODUCTION

Liquid crystal displays are considered as promising candidates to be used in future information systems. The information rate to be displayed by liquid crystals is limited by the multiplexing capability of the display. In order to display a high information rate for a wide range of viewing angles, electro-optic effects with a strong non-linearity of the electro-optic characteristics are required.

The most useful electro-optic effects are based on light scattering or on light absorption by polarizers or by dissolved dyes. There is no considerable mass-production of displays based on light scattering effects but there are some engineering models using Dynamic Scattering (DS) or the Cholesteric Nematic Phase Transition. Electro-optic effects which belong to the second group are Tunable Birefringence, the Twisted Nematic effect (TN), and the Guest-Host effect.

† Invited lecture presented at the Eighth International Liquid Crystal Conference, Kyoto, Japan, June 30–July 4, 1980.

During the past, the most useful candidate for applications in wristwatch and calculator displays was the TN-effect. Displays based on this effect are now considered for application in other areas such as consumer electronics, telecommunication, and automotive dashboards. TN-displays have been achieving great popularity as low voltage, low power devices designed as reflective, transflective, and transmissive displays. At present the most serious disadvantages are the limited multiplexing capability and the restricted temperature range. A considerable improvement should be attainable if material and cell parameters are optimized.

THEORY

If an electric field is applied to a TN cell with a twist of 90° and pretilt angle of 0° the deformation starts at the well-known threshold voltage[1]

$$V_0 = \pi\left(\frac{K_{11} + (K_{33} - 2K_{22})/4}{\varepsilon_0 \Delta_\varepsilon}\right)^{1/2}$$

Somewhat above this voltage, the cell becomes transparent in the case of parallel polarizers and non-transparent in the case of crossed polarizers. The optical response is a complicated function of material and cell parameters.

From a theoretical point of view, it seems reasonable first to calculate the tilt (α) and twist (β) angles in a sequence of sublayers as a function of the applied voltage, and second, the optical transmission for different angles of observation.[2–4] A definition of these angles is given in Figure 1. The deformation profile is dependent on the dielectric constants $\varepsilon_\parallel$ and $\varepsilon_\perp$, the elastic constants for splay, twist and bend K_{11}, K_{22}, K_{33}, the total twist $\beta = (90° - 2\beta_0)$, the tilt angle at the surface of the substrates α_0, and the applied voltage. The optical response depends in addition on the refractive indices n_e and n_0 and on the ratio of wavelength to cell thickness λ/d. For display applications, a finite tilt at the surfaces is required to avoid areas of opposite tilt. Therefore the deformation profiles are calculated for various combinations of K_{33}/K_{11}, $\Delta\varepsilon/\varepsilon_\perp$ and α_0, using Berreman's program. All calculations are performed for 10 μm cells and a pretilt $\alpha_0 = 1°$.

RESULTS

Results are shown in Figure 2(a) and (b). The tilt and twist angles α and β are plotted as functions of position within the liquid crystal layer. In Figure 2(a), the curve parameter is the reduced voltage V/V_0 while $\Delta\varepsilon/\varepsilon_\perp$ is kept constant. Solid and dashed lines are calculated with $K_{33}/K_{11} = 1.5$ and $K_{33}/K_{11} = 0.5$ respectively. Note that for V/V_0 near to and greater than unity, the tilt is increasing with decreasing K_{33}/K_{11}. A similar plot for a fixed

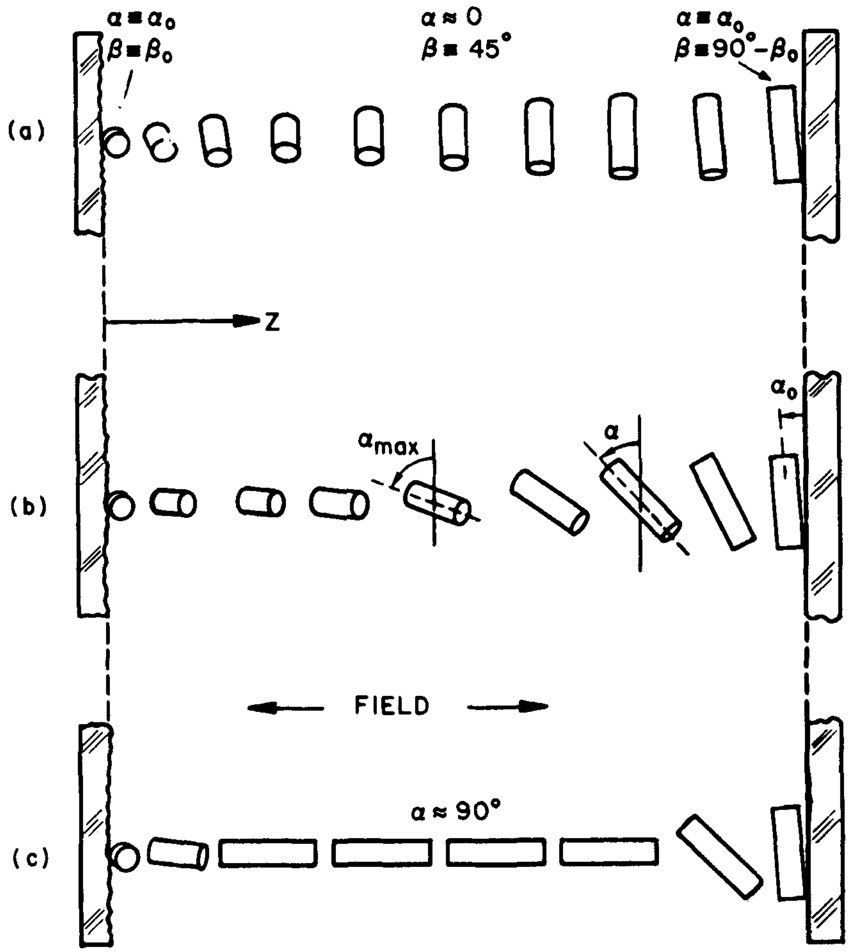

FIGURE 1 Diagram of the orientation of the liquid crystal axis in a cell (a) with no applied field, (b) with about twice the critical field, and (a) with several times the critical field. Note slight permanent tilt (α_0) and turn (β_0) at the surfaces.

K_{33}/K_{11} is presented in Figure 2(b). The curve parameter is $\Delta\varepsilon/\varepsilon_\perp$. In the case of larger $\Delta\varepsilon/\varepsilon_\perp$, a larger V/V_0 is necessary in order to achieve a comparable tilt α in the centre of the cell. Note, that the half width of the α-curves is larger for large $\Delta\varepsilon/\varepsilon_\perp$, while the shape of the β-curves is not too much affected.

In Figure 3(a) and (b) an angle in the centre of the cell and another one near the surface are plotted as a function of the applied voltage. In Figure 3(a), the parameter is K_{33}/K_{11}. It is obvious that the deformation is larger for smaller K_{33}/K_{11} at the same reduced voltage. If $\Delta\varepsilon/\varepsilon_\perp$ is the curve parameter and if

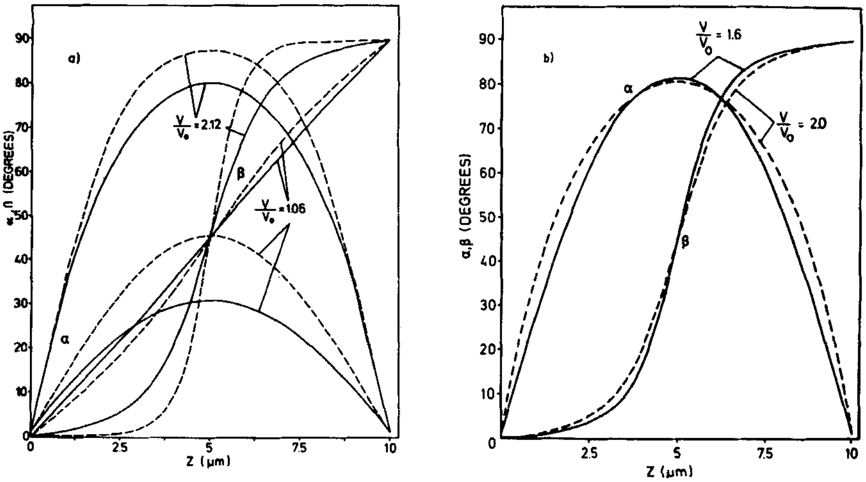

FIGURE 2a Tilt (α) and twist (β) angle as functions of the position z within the layer for a 10 μm cell. Solid lines: $K_{11} = 10.87 \cdot 10^{-12}$ N, $K_{22} = 9.5 \cdot 10^{-12}$ N, $K_{33} = 15.37 \cdot 10^{-12}$ N, dashed lines: $K_{11} = 10.87 \cdot 10^{-12}$ N, $K_{22} = 4.0 \cdot 10^{-12}$ N, $K_{33} = 5.0 \cdot 10^{-12}$ N. The ratio of $\Delta\varepsilon/\varepsilon_{\perp} = 0.05$.

FIGURE 2b Tilt (α) and twist (β) angle as functions of the position z within the layer for a 10 μm cell. Solid lines: $\Delta\varepsilon/\varepsilon_{\perp} = 0.05$; $V/V_0 = 1.6$; dashed line $\Delta\varepsilon/\varepsilon_{\perp} = 3.7$; $V/V_0 = 2.0$. The ratio of K_{33}/K_{11} is 0.5.

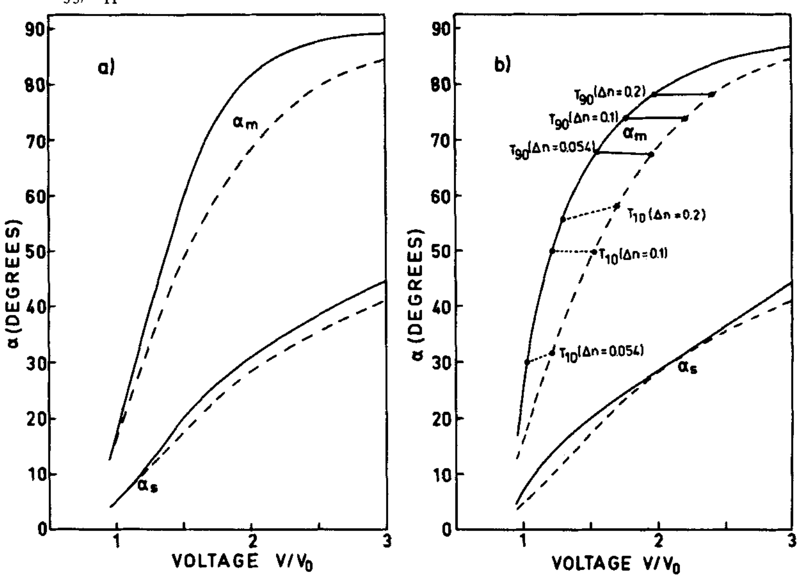

FIGURE 3 Tilt angle α_m in the centre and α_s about a quarter of the way from the surface as functions of the reduced voltage V/V_0. In Fig. 3(a), the curves are calculated with $\varepsilon_{\parallel} = 25.4$, $\varepsilon_{\perp} = 5.4$. The parameter K_{33}/K_{11} is 0.5 for the solid line and 1.5 for the dashed line. In Figure 3(b), the curves are calculated with $K_{33}/K_{11} = 1.5$. The parameters for the solid lines are $\varepsilon_{\parallel} = 10.5$, $\varepsilon_{\perp} = 10.0$, and $\varepsilon_{\parallel} = 25.4$, $\varepsilon_{\perp} = 5.4$ for the dashed lines.

K_{33}/K_{11} is kept constant, the deformation in the centre of the cell is larger for smaller $\Delta\varepsilon/\varepsilon_\perp$ at the same V/V_0. This is shown in Figure 3(b).

With these sets of angles, the optical transmission curves are calculated for different combinations of parameters. Curves for normal incidence are presented in Figure 4. In the upper part the curve parameter is K_{33}/K_{11}. The transmission characteristics are steepest for the smallest values of K_{33}/K_{11}, as expected from the director distribution. In the lower part, the curve parameter is $\Delta\varepsilon/\varepsilon_\perp$. The significant value V_{90}/V_{10} of the characteristics is smallest for largest $\Delta\varepsilon/\varepsilon_\perp$. This is the more pronounced the larger K_{33}/K_{11}. Note, that this is true only in the case of normal incidence.

The result can be understood easily by regarding again the tilt angles α in the centre of the cell that are plotted in Figure 3. As expected, the tilt angles correlated with 10% transmission (T_{10}) as well as those correlated with 90% transmission (T_{90}) are nearly independent of the value of $\Delta\varepsilon/\varepsilon_\perp$. Therefore

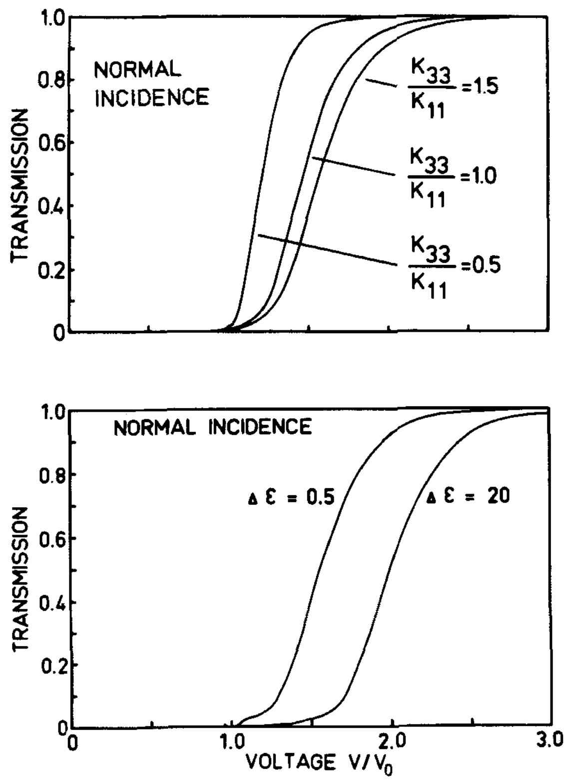

FIGURE 4 Optical transmission of a TN-cell between parallel polarizers for normal incidence, calculated with $n_e = 1.728$ and $n_0 = 1.523$. In the upper part $\varepsilon_\parallel = 10.5$ and $\varepsilon_\perp = 10.0$ in the lower part $K_{33}/K_{11} = 1.5$.

the ratio V_{90}/V_{10} of the transmission characteristics is mainly dependent on the shape of the α_m-curves between about 30° and 80°.

This is confirmed by the shapes of the director distributions for different $\Delta\varepsilon/\varepsilon_\perp$ as shown in Figure 2(b). For comparable tilts α_m in the centre of the cell, tne distribution over the cell thickness is quite similar. The slight difference should not influence the optical characteristics considerably.

To characterize the performance of a display, it is necessary to know the transmission for a large range of viewing angles.[5–13] Therefore the transmission curves for six different viewing angles in four different planes of observation are evaluated. The viewing angles are characterized by the off-axis angle θ and an angle φ defined by the plane of observation and the plane containing the director in the centre of the cell and the z-axis, as shown in Figure 5.

Transmission curves are calculated for $\theta = 45°$ with $\varphi = 0°, 45°, 90°, 135°, 180°, 225°, 270°, 315°$.

Results are shown in Figure 6. K_{33}/K_{11} is 1.5 in the upper part and 0.5 in the lower part. It is obvious that the slopes become steeper for smaller values of K_{33}/K_{11} and in addition, the distance between curves for normal incidence ($\theta = 0°$, $\varphi = 0°$) and off-axis incidence ($\theta = 45°$, $\varphi = 180°$) becomes smaller.

In Figure 7 results are plotted for $K_{33}/K_{11} = 1.5$ while $\Delta\varepsilon/\varepsilon_\perp = 3.7$ in the upper part and $\Delta\varepsilon/\varepsilon_\perp = 0.05$ in the lower part. For normal incidence, the slopes of the transmission curves become a little bit steeper or do not change significantly due to the variation of $\Delta\varepsilon/\varepsilon_\perp$ ranging from 0.05 to 3.7. The extent of this change is in addition governed by the ratio of K_{33}/K_{11}.

Nevertheless, for large $\Delta\varepsilon/\varepsilon_\perp$, these curves are shifted towards higher values

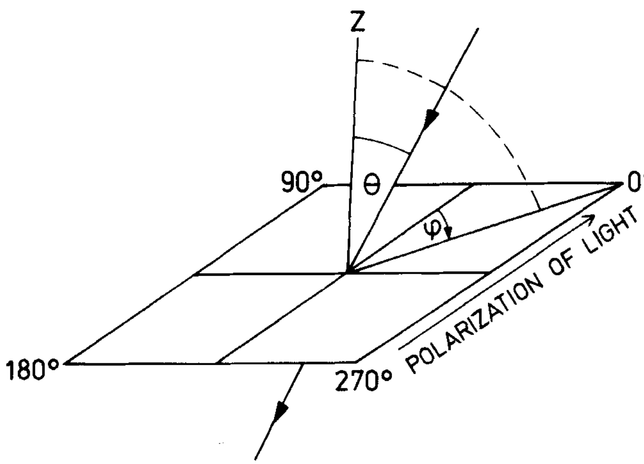

FIGURE 5 Schematic diagram to explain the viewing angles, chosen for the calculation of the transmission characteristics. θ is the off-axis angle; φ the angle between the plane of polarisation of incident light and the plane of observation.

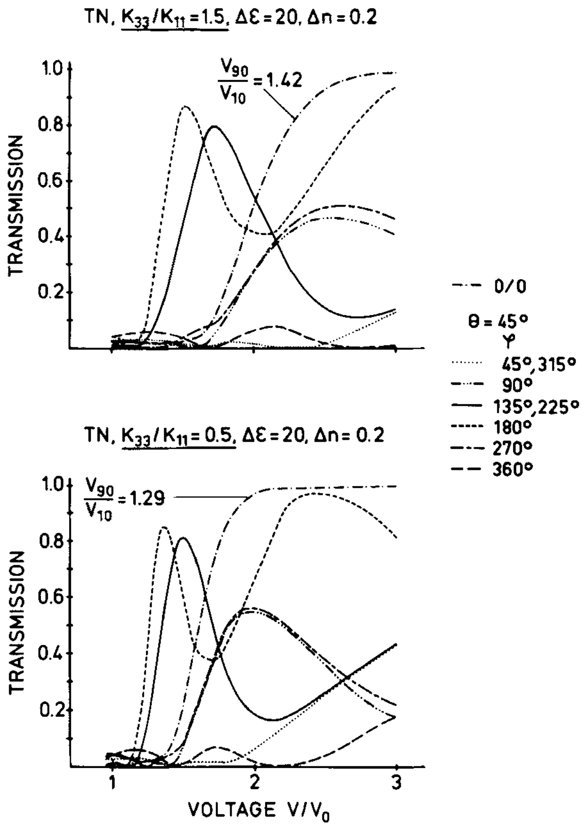

FIGURE 6 Transmission characteristics of a TN-cell, calculated with $\varepsilon_{\parallel} = 25.4$, $\varepsilon_{\perp} = 5.4$; $n_e = 1.728$, $n_0 = 1.528$; $\lambda = 632.8$ nm; $d = 10\ \mu$m. Upper part: $K_{33}/K_{11} = 1.5$; Lower part: $K_{33}/K_{11} = 0.5$.

of V/V_0 and the distance between curves for normal incidence ($\theta = 0$, $\varphi = 0$) and off-axis incidence ($\theta = 45°$, $\varphi = 180°$) becomes larger.

Results calculated with fixed K_{33}/K_{11} as well as fixed $\Delta\varepsilon/\varepsilon_{\perp}$, but with a Δn ranging from 0.2 to 0.1, are given in Figure 8. For smaller Δn, the transmission curves are steeper and in addition the well known bounce is less pronounced, but there is a residual transparency of about 10% in the off-state.

In the previous part of this paper, only a classic Twisted Nematic Cell in the limits of the Mauguin approximation is considered. In this approximation the inequality

$$d \times \Delta n \gg \frac{\lambda}{2}$$

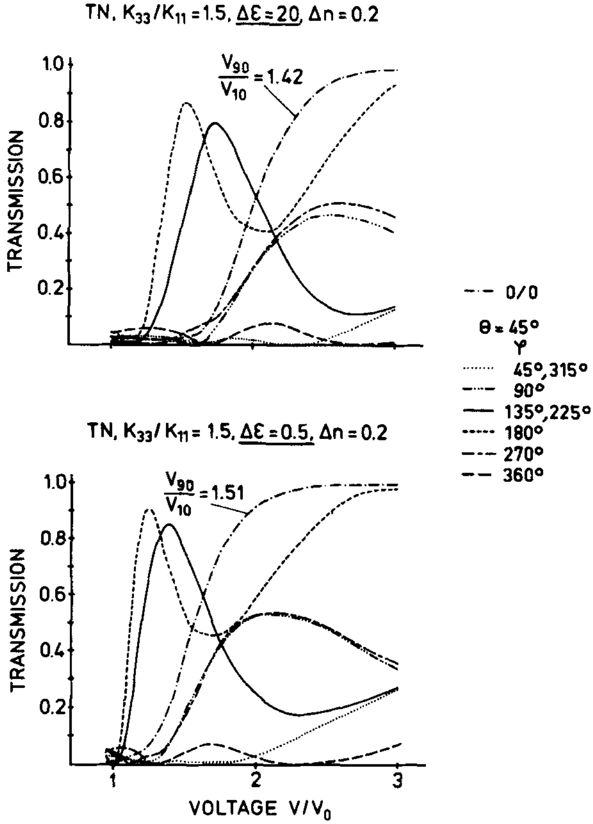

FIGURE 7 Transmission charactzristics of a TN-cell calculated with $K_{33}/K_{11} = 1.5$: $n_e = 1.728$, $n_0 = 1.528$; $\lambda = 632.8$ nm; $d = 10$ μm. Upper part: $\varepsilon_{\parallel} = 25.4$, $\varepsilon_{\perp} = 5.4$; Lower part: $\varepsilon_{\parallel} = 10.5$, $\varepsilon_{\perp} = 10.0$.

must be satisfied in order that light waves travelling through a TN cell are linearly polarized.

If this inequality is not satisfied—for smaller $d \times \Delta n$—plane polarized light emerges elliptically polarized when transmitted through the cell. The optical properties of such structures have been considered by a number of authors. A closed solution for the light intensity transmitted through a structure with a pitch small compared with the cell thickness has been given by Gooch and Tarry.[14] If both polarizer and analyser are parallel to the director at the first surface the transmitted intensity is

$$T = \frac{\sin^2[\pi/2(1 + u^2)^{1/2}]}{(1 + u^2)}$$

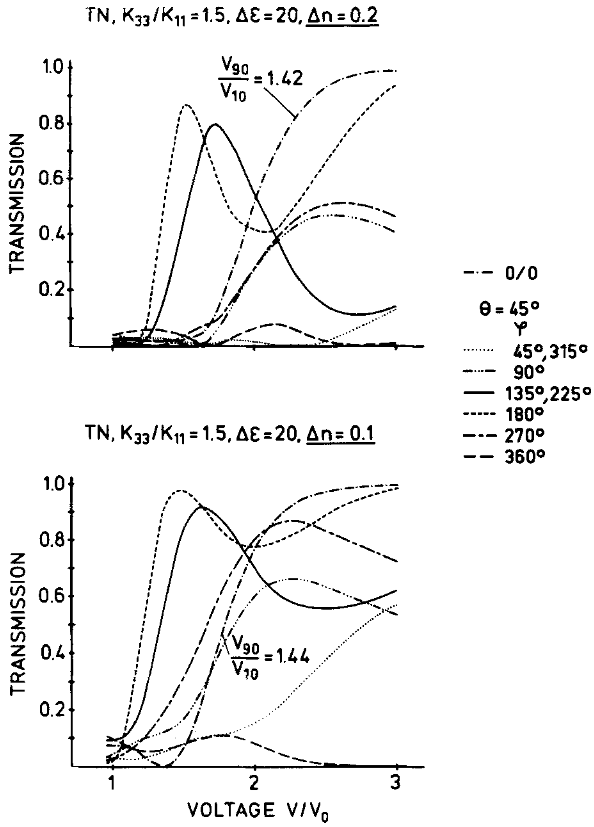

FIGURE 8 Transmission characteristics of a TN-cell. Calculated with $K_{33}/K_{11} = 1.5$: $\varepsilon_{\parallel} = 25.4$, $\varepsilon_{\perp} = 5.4$, $\lambda = 632.8$ nm; $d = 10\ \mu$m. Upper part: $n_e = 1.728$, $n_0 = 1.528$; Lower part: $n_e = 1.62$, $n_0 = 1.52$.

with

$$u = 2 \times d \times \frac{\Delta n}{\lambda}$$

There are minima in transmission for

$$u = 2 \times d \times \Delta n/\lambda = \sqrt{3},\ \sqrt{15},\ \sqrt{35},\ \sqrt{63}\ \ldots$$

as shown in Figure 9.

In contrast to the Mauguin approximation, the transmitted intensity in the off-state is a minimum for discrete combinations of d, Δn, and λ only.

The calculated transmission characteristics of TN-cells presented before indicate that the optical characteristics in the on-state can be improved con-

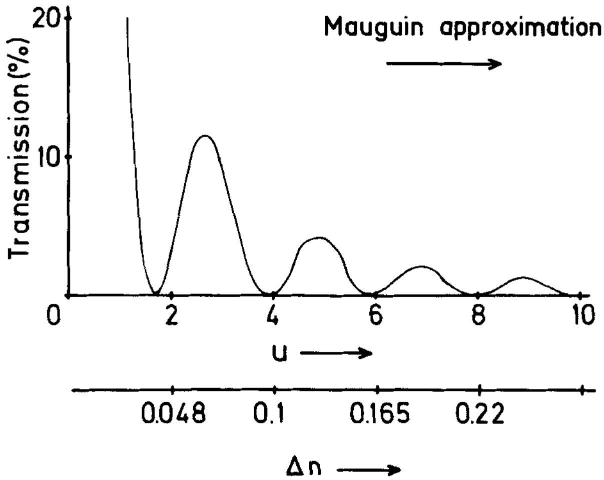

FIGURE 9 Transmission of a twisted nematic structure as a function of $u = 2d\,\Delta n/\lambda$. Second scale (Δn) is calculated with $d = 10$ μm and $\lambda = 550$ nm.

siderably by minimizing the product of $d \times \Delta n$. Therefore we calculated transmission curves as a function of the applied voltage for a 10 μm cell with $\Delta n = 0.054$. This combination of cell thickness and Δn corresponds to the first transmission minimum in the off-state centred at $\lambda = 632.8$ nm. Results are plotted in the lower part of Figure 10. The corresponding curves calculated with $\Delta n = 0.2$ are given in the upper part. There is no significant change in the steepness of the slope for normal incidence, but the off-axis transmission is improved considerably.

To illustrate the transmitted intensity for a large range of viewing angles, curves have been evaluated for an off-axis angle $\theta = 45°$ and the azimuthal angles φ in steps of 10° with $K_{33}/K_{11} = 1.5$, $\Delta\varepsilon = 20$, and Δn ranging from 0.2 to 0.054. Results, calculated with 4 different reduced voltages, are plotted in Figure 11. The dashed lines are calculated with $\Delta n = 0.2$ and 0.1 respectively. The solid line is calculated with $\Delta n = 0.054$.

Corresponding curves are obtained for $K_{33}/K_{11} = 0.5$ and $\Delta\varepsilon = 0.5$. It is obvious that for any combination of material parameters and any reduced voltage the range of observation angles is considerably improved, if the product of cell thickness d and Δn is adapted to the first transmission minimum in the off-state.

In order to check the wavelength-dependence of the optical characteristics, transmission curves are calculated with $\lambda = 632.8$ nm and 450 nm for a reduced voltage $V/V_0 = 3$ and for the off-state. Results, given in Figure 12, indicate that the transmission is not too much different for wavelengths ranging from 650 nm to 450 nm.

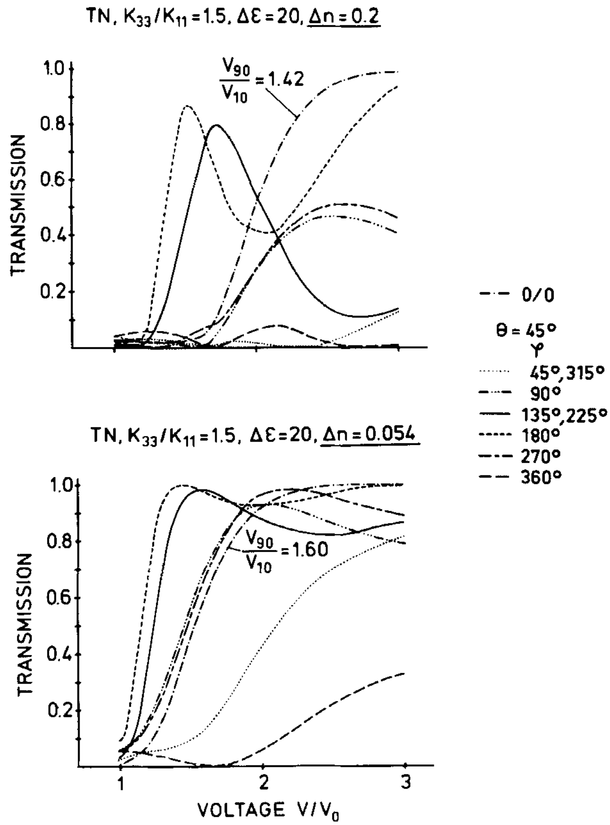

FIGURE 10 Transmission characteristics of a TN-cell calculated with $K_{33}/K_{11} = 1.5$, $\varepsilon_{\parallel} = 25.4$, $\varepsilon_{\perp} = 5.4$; $\lambda = 632.8$ nm; $d = 10\ \mu$m. Upper part: $n_e = 1.728$, $n_0 = 1.528$; Lower part: $n_e = 1.534$, $n_0 = 1.48$.

Two other configurations, a 90° twist cell and a homogeneous planar cell, both with polarizer and analyser oriented at 45° to the director at the first surface, are also investigated. Results are given in Figure 13, together with the TN configuration. Cell thickness and Δn are again adjusted to achieve the first transmission minimum in the off-state. The results indicate that the optical characteristics cannot be improved considerably using one of these configurations.

In display applications a serious problem is the appearance of coloured areas in the off-state. Therefore it seems reasonable to compare the wavelength dependence of the transmission for the different configurations discussed before. Transmission curves for normal incidence are plotted in Figure 14 for a TN cell with $\Delta n = 0.2$, 0.1, 0.048 and a twist cell, as well as for a homogeneous planar cell with polarizers oriented at an angle of 45° to

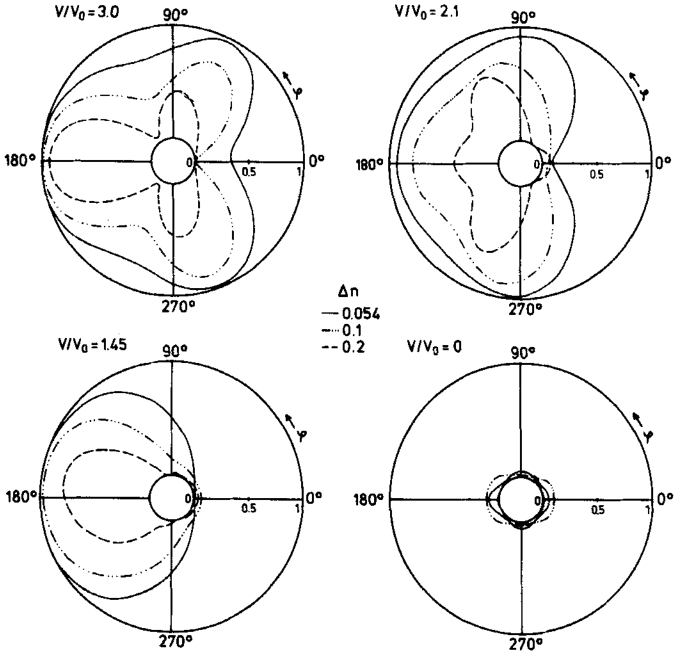

FIGURE 11 Transmission characteristics ($\theta = 45°$) of a TN-cell, calculated with $K_{33}/K_{11} = 1.5$, $\varepsilon_{\parallel} = 25.4$, $\varepsilon_{\perp} = 5.4$, $d = 10\ \mu m$, $\lambda = 632.8$ nm. Parameter is Δn.

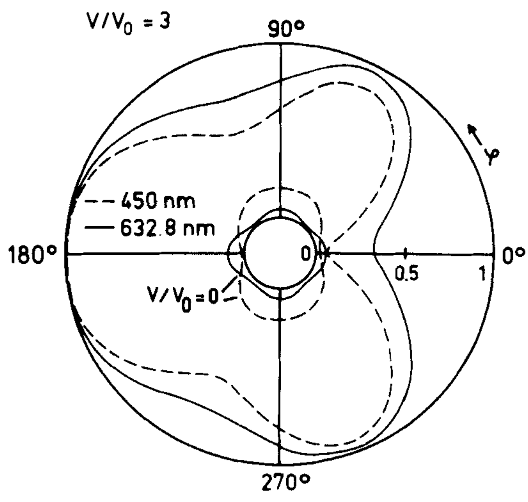

FIGURE 12 Transmission characteristics ($\theta = 45°$) of a TN-cell, calculated with $K_{33}/K_{11} = 1.5$, $\varepsilon_{\parallel} = 25.4$, $\varepsilon_{\perp} = 5.4$, $d = 10\ \mu m$, $n_e = 1.534$, $n_0 = 1.48$. Parameter is the wavelength.

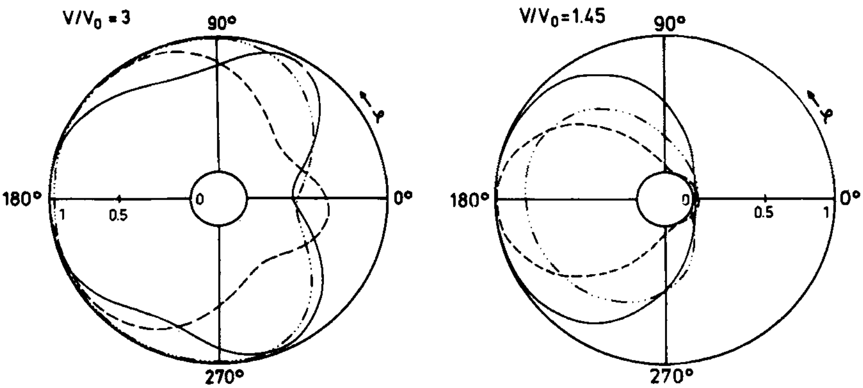

FIGURE 13 Transmission characteristics ($\theta = 45°$) calculated with $K_{33}/K_{11} = 1.5$, $\varepsilon_{\parallel} = 25.4$, $\varepsilon_{\perp} = 5.4$, $d = 10\ \mu m$, $\lambda = 632.8$ nm. Solid line: — for a TN configuration $\Delta n = 0.054$. Polarizers are parallel to the director and the first surface. Dashed lines: -- for a TN configuration $\Delta n = 0.054$. -··· - for a homogeneous planar configuration $\Delta n = 0.031$. Polarizers are oriented at 45° to the director at the first surface.

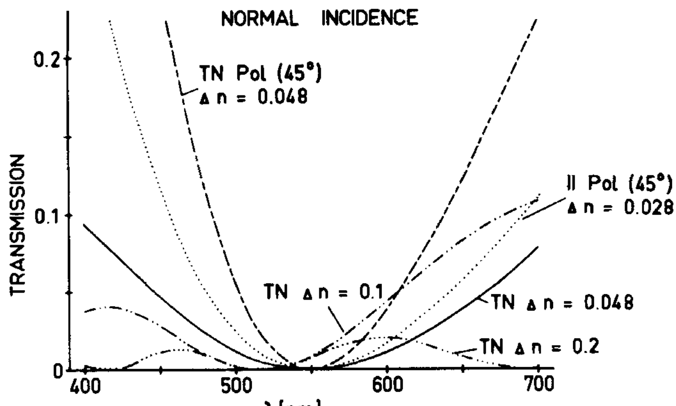

FIGURE 14 Optical transmission of different configurations between parallel polarizers. —····— TN ($\Delta n = 0.2$), —··— TN ($\Delta n = 0.1$), —— TN ($\Delta n = 0.048$); polarizers are parallel to the director at the first surface, — — — TN ($\Delta n = 0.048$); polarizers are oriented 45° to the director at the first surface.········· Homogeneous planar ($\Delta n = 0.028$); polarizers are oriented 45° to the director at the first surface.

the director at the first surface. It is obvious that the wavelength dependence is less pronounced for the TN configuration.

The results are summarized in Table I. From a theoretical point of view the optical characteristic of a TN-display can be optimized by using a material with small K_{33}/K_{11}, large K_{33}/K_{22} and $\Delta\varepsilon/\varepsilon_{\perp}$, that is not larger than required by the given addressing scheme. In addition the combination of cell thickness and Δn should be matched to the first transmission minimum in the centre of the visible wavelength range.

TABLE I

Calculated optical performance $V_{90}\%$ transmission $(\theta, \varphi)V_{10}\%$ transmission (θ, ψ) for different combinations of K_{33}/K_{11}, $\Delta\varepsilon/\varepsilon_{\perp}$, Δn. The cell $d = 10\ \mu m$; the pretilt $\alpha_0 = 1^{\circ}$.

		$\Delta n = 0.2$			$\Delta n = 0.1$			$\Delta n = 0.054$		
$\frac{K_{33}}{K_{11}}$	$\frac{\Delta\varepsilon}{\varepsilon_{\perp}}$	$\frac{V_{90(0.0)}}{V_{10(0.0)}}$	$\frac{V_{90(0.0)}}{V_{10(180)}}$	$\frac{V_{50(0.0)}}{V_{10(180)}}$	$\frac{V_{90(0.0)}}{V_{10(0.0)}}$	$\frac{V_{90(0.0)}}{V_{10(180)}}$	$\frac{V_{50(0.0)}}{V_{10(180)}}$	$\frac{V_{90(0.0)}}{V_{10(0.0)}}$	$\frac{V_{90(0.0)}}{V_{10(180)}}$	$\frac{V_{50(0.0)}}{V_{10(180)}}$
1.5	3.7	1.42	1.95	1.60	1.44	1.98	1.66	1.60	1.95	1.51
1.5	0.05	1.51	1.85	1.48	1.45	1.77	1.43	1.52	1.56	1.25
0.5	3.7	1.29	1.59	1. 8	1.28	1.53	1.37	1.40	1.60	1.38
0.5	0.05	1.32	1.42	1.21	1.25	1.32	1.20	1.22	1.22	1.11

Acknowledgement

The author wishes to thank D. W. Berreman for supplying us with computer program, W. Fehrenbach for performing calculations, L. Pohl for valuable suggestions concerning low Δn-materials and G. Meier, B. Scheuble, and A. Stieb for helpful discussions.

References

1. M. Schadt and W. Helfrich, *Appl. Phys. Lett.*, **18**, 127 (1971).
2. C. Z. van Doorn, *J. Appl. Phys.*, **46**, 3738 (1975).
3. D. W. Berreman, *J. Appl. Phys.*, **46**, 3746 (1975).
4. F. Gharadjedaghi and J. Robert, *Rev. Phys. Appliquée*, **11**, 467 (1976).
5. A. R. Kmetz, *1978 SID Int. Symposium, Digest*, p. 70.
6. P. A. Penz, *1978 SID Int. Symposium, Digest*, p. 68.
7. G. Baur, F. Windscheid, and D. W. Berreman, *Appl. Phys.*, **8**, 101 (1975).
8. G. Baur, in *The Physics and Chemistry of Liquid Crystal Devices*, Plenum Press, New York (1980), pp. 61–78.
9. F. J. Kahn and H. Birecki, in *The Physics and Chemistry of Liquid Crystal Devices*, Plenum Press, New York (1980), pp. 79–93.
10. C. Z. van Doorn, C. J. Gerritsma, and J. J. M. J. de Klerk, in *The Physics and Chemistry of Liquid Crystal Devices*, Plenum Press, New York (1980), pp. 95–104.
11. H. Birecki and F. J. Kahn, in *The Physics and Chemistry of Liquid Crystal Devices*, Plenum Press, New York (1980), pp. 125–142.
12. J. Nehring, *Third Liq. Cryst. Conf., Budapest*, Aug. 1979.
13. E. P. Raynes, *Proceedings of the SID*, **20**, 189 (1979).
14. C. H. Gooch and H. A. Tarry, *J. Phys. D, Appl. Phys.*, **8**, 1575 (1975).